Stochastic and Resolvable Gravitational Waves from Ultralight Bosons

Richard Brito,[1] Shrobana Ghosh,[2] Enrico Barausse,[3] Emanuele Berti,[2,4] Vitor Cardoso,[4,5] Irina Dvorkin,[3,6]
Antoine Klein,[3] and Paolo Pani[7,4]

[1]*Max Planck Institute for Gravitational Physics (Albert Einstein Institute),*
Am Mühlenberg 1, Potsdam-Golm 14476, Germany
[2]*Department of Physics and Astronomy, The University of Mississippi, University, Mississippi 38677, USA*
[3]*Institut d'Astrophysique de Paris, Sorbonne Universités,*
UPMC Univ Paris 6 & CNRS, UMR 7095, 98 bis bd Arago, 75014 Paris, France
[4]*CENTRA, Departamento de Física, Instituto Superior Técnico,*
Universidade de Lisboa, Avenida Rovisco Pais 1, 1049 Lisboa, Portugal
[5]*Perimeter Institute for Theoretical Physics, 31 Caroline Street North Waterloo, Ontario N2L 2Y5, Canada*
[6]*Institut Lagrange de Paris (ILP), Sorbonne Universités, 98 bis bd Arago, 75014 Paris, France*
[7]*Dipartimento di Fisica, "Sapienza" Università di Roma & Sezione INFN Roma1,*
Piazzale Aldo Moro 5, 00185 Roma, Italy
(Received 23 June 2017; revised manuscript received 31 August 2017; published 27 September 2017)

Ultralight scalar fields around spinning black holes can trigger superradiant instabilities, forming a long-lived bosonic condensate outside the horizon. We use numerical solutions of the perturbed field equations and astrophysical models of massive and stellar-mass black hole populations to compute, for the first time, the stochastic gravitational-wave background from these sources. In optimistic scenarios the background is observable by Advanced LIGO and LISA for field masses m_s in the range $\sim [2 \times 10^{-13}, 10^{-12}]$ and $\sim 5 \times [10^{-19}, 10^{-16}]$ eV, respectively, and it can affect the detectability of resolvable sources. Our estimates suggest that an analysis of the stochastic background limits from LIGO O1 might already be used to marginally exclude axions with mass $\sim 10^{-12.5}$ eV. Semicoherent searches with Advanced LIGO (LISA) should detect $\sim 15(5)$ to 200(40) resolvable sources for scalar field masses 3×10^{-13} (10^{-17}) eV. LISA measurements of massive BH spins could either rule out bosons in the range $\sim [10^{-18}, 2 \times 10^{-13}]$ eV, or measure m_s with 10% accuracy in the range $\sim [10^{-17}, 10^{-13}]$ eV.

Introduction.—The historic LIGO gravitational wave (GW) detections [1–3] provide the strongest evidence to date that astrophysical black holes (BHs) exist and merge [4–6]. Besides probing the nature of compact objects and testing general relativity [7–10], LIGO [11], and the space-based detector LISA [12] may revolutionize our understanding of particle physics and dark matter. Ultralight bosons, which could be a significant component of dark matter [13–16], interact very weakly (if at all) with baryonic matter, but the equivalence principle implies that their gravitational interaction should be universal. Low-energy bosons near spinning BHs can trigger a superradiant instability whenever the boson frequency ω_R satisfies the superradiant condition $0 < \omega_R < m\Omega_H$, where Ω_H is the horizon angular velocity and m is an azimuthal quantum number, with possible astrophysical implications [17–20].

Despite extensive work on massive spin-0 [18,21–23], spin-1 [24–29], and spin-2 fields [30], the evolution and the end state of the instability are not fully understood [31–34]. Recent numerical simulations [28] support the conclusions of perturbative studies [20,29,35–39]: the BH spins down, transferring energy and angular momentum to a mostly dipolar boson condensate until $\omega_R \sim m\Omega_H$. The energy scale is set by the boson mass $m_s \equiv \mu\hbar$, which implies that $\omega_R \sim \mu$

and that the instability saturates at $\mu \sim m\Omega_H$ (in units $G = c = 1$). The condensate is then dissipated through the emission of mostly quadrupolar GWs, with frequency set by μ. The mechanism is most effective when the boson's Compton wavelength is comparable to the BH's gravitational radius: detailed calculations show that the maximum instability rate for scalar fields corresponds to $M\mu \simeq 0.42$ [23]. Therefore, the instability window corresponds to masses $m_s \sim 10^{-14} - 10^{-10}$ and $m_s \sim 10^{-19} - 10^{-15}$ eV for LIGO and LISA BH-boson condensate sources, respectively [20]. In this work and in a companion paper [40] we argue that GW detectors can discover new particles beyond the standard model or impose constraints on their masses.

GWs from scalar condensates around BHs.—The instability occurs in two stages [36]. In the first (linear) phase the condensate grows on a time scale $\tau_{\rm inst} \sim M^{-8}\mu^{-9}$ until the superradiant condition is nearly saturated. In the second (nonlinear) phase GW emission governs the evolution of the condensate, which is dissipated over a time scale $\tau_{\rm GW}$ that depends on its mass M_S and on the GW emission rate. These two time scales can be computed analytically when $M\mu \ll 1$ [40]. For small dimensionless BH spins $\chi \equiv J/M^2 \ll 1$, they read

$$\tau_{\rm inst} \sim 0.07 \chi^{-1} \left(\frac{M}{10\,M_\odot}\right) \left(\frac{0.1}{M\mu}\right)^9 \; {\rm yr}, \qquad (1)$$

$$\tau_{\rm GW} \sim 6 \times 10^4 \chi^{-1} \left(\frac{M}{10\,M_\odot}\right) \left(\frac{0.1}{M\mu}\right)^{15} \; {\rm yr}. \qquad (2)$$

These relations (valid for any BH mass) are a good approximation even when $M\mu$ and χ are ~ 1 [40]. Since $\tau_{\rm GW} \gg \tau_{\rm inst} \gg M$, the condensate has enough time to grow, and the evolution of the system can be studied in a quasiadiabatic approximation [36] using Teukolsky's formalism [41,42]. The field's stress-energy tensor is typically small; thus, its backreaction is negligible [28,36].

Over the emission time scale (which in most cases is much longer that the observation time $T_{\rm obs}$), the GWs are nearly monochromatic, with frequency $f_s = \omega_R/\pi \sim \mu/\pi$. As such, BH-boson condensates are continuous sources, like pulsars for LIGO or verification binaries for LISA. We conservatively assume that GWs are produced after saturation of the instability, which leads the BH from an initial state (M_i, J_i) to a final state (M, J), and we thus compute the root-mean-square strain amplitude h using the *final* BH parameters. By averaging over source and detector orientations we get

$$h = \sqrt{\frac{2}{5\pi}} \frac{GM}{c^2 r} \left(\frac{M_S}{M}\right) A(\chi, f_s M), \qquad (3)$$

where r is the (comoving) distance to the source, the masses are in the source frame, and the dimensionless function $A(\chi, f_s M)$ is computed from BH perturbation theory [40,42]. Our results are more accurate than the analytic approximations of [35,36]. It can be shown that M_S scales linearly with J_i [40], so h also grows with J_i. For LISA, we also take into account correction factors due to the detector geometry [43]. In the detector frame, Eq. (3) still holds if the masses M and M_S are multiplied by $(1 + z)$, r is replaced by the luminosity distance, and the frequency is replaced by the detector-frame frequency $f = f_s/(1 + z)$. Nevertheless, one needs to use detector-frame frequencies when comparing to the detector sensitivity.

In semicoherent searches of monochromatic sources, the signal is divided in $\mathcal{N}$ coherent segments of time length $T_{\rm coh}$, and we have $h_{\rm thr} \simeq 25 \mathcal{N}^{-1/4} \sqrt{S_h(f)/T_{\rm coh}}$, where $h_{\rm thr}$ is the minimum root-mean-square strain amplitude detectable over the observation time $\mathcal{N} \times T_{\rm coh}$ [44], and $S_h(f)$ is the noise power spectral density (PSD) at f [45].

In Fig. 1 we compare the GW strain of Eq. (3) with the PSDs of LISA and Advanced LIGO at design sensitivity. The GW strain increases almost vertically as a function of $\omega_R \simeq \mu$ in the superradiant range $(0, \Omega_H)$. Thin solid curves correspond to the stochastic background from the whole BH population, for a boson mass m_s. This background produces a "confusion noise" when $m_s \approx [10^{-18}, 10^{-16}]$ eV, complicating the detection of individual sources. Figure 1 suggests
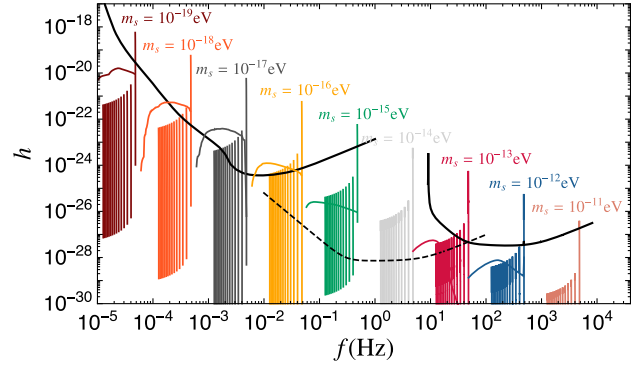

FIG. 1. GW strain produced by BH-boson condensates compared to the Advanced LIGO PSD at design sensitivity [46] and to the nonsky averaged LISA PSD [12] (black thick curves), assuming a coherent observation time of $T_{\rm obs} = 4$ yr in both cases. Nearly vertical lines represent BHs with initial spin $\chi_i = 0.9$. Each line corresponds to a single source at redshift $z \in (0.001, 3.001)$ (from right to left, in steps of $\delta z = 0.2$), and different colors correspond to different boson masses m_s. Thin lines show the stochastic background produced by the whole population of astrophysical BHs under optimistic assumptions (cf. main text for details). The PSD of DECIGO [47] (dashed line) is also shown for reference.

that bosons with masses 10^{-19} eV $\lesssim m_s \lesssim 10^{-11}$ eV (with a small gap around $m_s \sim 10^{-14}$ eV, which might be filled by DECIGO [47]) could be detectable by LIGO and LISA. Below we quantify this expectation.

BH population models.—Assessing the detectability of these signals requires astrophysical models for BH populations. For LISA sources, the main uncertainties concern the mass and spin distribution of isolated BHs, the model for their high-redshift seeds, and their accretion and merger history. We adopt the same populations of Refs. [48,49], which were based on the semianalytic galaxy formation calculations of Ref. [50] (see also Refs. [51–53]). In our *optimistic* model, we use these calculations to infer the redshift-dependent BH number density $d^2 n/(d\log_{10} M d\chi)$. The spin distribution is skewed toward $\chi_i \sim 1$, at least at low masses [51]. We also adopt less optimistic and pessimistic models with mass function given by Eqs. (5) and (6) of Ref. [49] for $z < 3$ and $10^4\,M_\odot < M < 10^7\,M_\odot$, whereas for $M > 10^7\,M_\odot$ we use a mass distribution with normalization 10 and 100 times lower than the optimistic one. In both the less optimistic and pessimistic models we assume a uniform spin distribution in the range $\chi_i \in [0, 1]$.

The LIGO stochastic GW background comes mostly from extragalactic stellar-mass BHs, which were ignored in previous work [37]. Here we model these sources using the semianalytic galaxy evolution model of Ref. [54]. The BH formation rate as a function of mass and redshift reads

$$\frac{d\dot{n}_{\rm eg}}{dM} = \int d\mathcal{M}_\star \psi[t - \tau(\mathcal{M}_\star)] \phi(\mathcal{M}_\star) \delta[\mathcal{M}_\star - g^{-1}(M)], \quad (4)$$

where $\tau(\mathcal{M}_\star)$ is the lifetime of a star of mass $\mathcal{M}_\star$, $\phi(\mathcal{M}_\star)$ is the stellar initial mass function, $\psi(t)$ is the cosmic star formation rate (SFR) density, and δ is the Dirac delta. We fit the cosmic SFR as described in Ref. [55] and calibrate it to observations of luminous galaxies [56,57]. We assume a Salpeter initial mass function $\phi(\mathcal{M}_\star) \propto \mathcal{M}_\star^{-2.35}$ [58] in the range $\mathcal{M}_\star \in [0.1 - 100]M_\odot$, and take stellar lifetimes from Ref. [59]. We also follow the production of metals by stars [60] and the resulting enrichment of the interstellar medium, which affects the metallicity of subsequent stellar generations. The function $g(\mathcal{M}_\star)$ relates the initial stellar mass $\mathcal{M}_\star$ and the BH mass M, and encodes the BH formation process. In general, the mass of the BH formed from a star with initial mass $\mathcal{M}_\star$ depends on the stellar metallicity [61] and rotational velocity [62], as well as interactions with its companion if the star belongs to a binary system. We assume that all stellar-mass BHs are produced from isolated massive stars after core collapse, and calculate the BH mass for a given $\mathcal{M}_\star$ and metallicity using the analytic fits for the "delayed" model of Ref. [63]. Through the metallicity, the function $M = g(\mathcal{M}_\star)$ is implicitly a function of redshift. Since this model does not predict the initial BH spins, we assume a uniform distribution and explore different ranges: $\chi_i \in [0.8, 1]$, $[0.5, 1]$, $[0, 1]$, and $[0, 0.5]$.

The dominant contribution to LIGO resolvable signals comes from Galactic stellar-mass BHs [37]. We estimate their present-day mass function as

$$\frac{dN_{\rm MW}}{dM} = \int dt \, \frac{{\rm SFR}(z)}{\mathcal{M}_\star} \frac{dp}{d\mathcal{M}_\star} \left| \frac{dM}{d\mathcal{M}_\star} \right|^{-1}, \qquad (5)$$

where the integration is over all cosmic times prior to the present epoch; $N_{\rm MW}$ denotes the number of BHs in the Galaxy; ${\rm SFR}(z)$ is the SFR of Milky-Way type galaxies as a function of redshift [57,64]; $dp/d\mathcal{M}_\star$ is the probability of forming a star with mass between $\mathcal{M}_\star$ and $\mathcal{M}_\star + d\mathcal{M}_\star$ (obtained from the Salpeter initial mass function); and $dM/d\mathcal{M}_\star$ is given by the delayed model of Ref. [63]. This latter quantity is a function of redshift through the metallicity, whose redshift evolution we model following Ref. [65]. To obtain a (differential) BH number density $dn_{\rm MW}/dM$, we "spread" this mass function over the Galaxy, proportionally to the (present) stellar density. For the latter we assume a simple bulge + disk model, where the bulge is modeled via a Hernquist profile [66] with mass $\sim 2 \times 10^{10} \, M_\odot$ and scale radius ~ 1 kpc [67], and the disk has an exponential profile with mass $\sim 6 \times 10^{10} \, M_\odot$ and scale radius ~ 2 kpc [68].

Stochastic background.—The stochastic background produced by BH-boson condensates is given by an integral over unresolved sources—those with signal-to-noise ratio (SNR) $\rho < 8$—of the formation rate density per comoving volume $\dot{n}$ [69]:

$$\Omega_{\rm GW}(f) = \frac{f}{\rho_c} \int_{\rho < 8} dz \frac{dt}{dz} \dot{n}(M, \chi, z) \frac{dE_s}{df_s}, \qquad (6)$$

where $\rho_c = 3H_0^2/(8\pi) \approx 1.3 \times 10^{11} \, M_\odot/{\rm Mpc}^3$ is the critical density of the Universe, dt/dz is the derivative of the lookback time $t(z)$ with respect to z, dE_s/df_s is the energy spectrum in the source frame, and f is the detector-frame frequency. For LIGO we compute $\dot{n}$ by integrating Eqs. (4) and (5). For LISA we integrate $d^2 n/(d \log_{10} M d\chi)$—as given by the aforementioned "optimistic," "less optimistic" and "pessimistic" models—with respect to mass and spin, and we assume that $\dot{n} = n/t_0$, where $t_0 \approx 13.8$ Gyr is the age of the Universe (i.e., each BH undergoes boson annihilation only once in its cosmic history). This assumption does not significantly affect our results, because subsequent annihilation signals (if they occur at all) are much weaker [40].

For the spectrum of the GW signal we assume $dE_s/df_s \approx E_{\rm GW}\delta[f(1+z) - f_s]$, where $E_{\rm GW}$ is the total energy radiated in GWs over the signal duration Δt, and the Dirac delta is "spread out" over a frequency window of width $\sim \max\{1/[\Delta t(1+z)], 1/T_{\rm obs}\}$ to account for the finite signal duration and observation time. For LIGO we can safely neglect the effect of mergers [70,71] and accretion [72]. For LISA, we conservatively assume that mergers and accretion cut the signal short, and thus define the signal duration as $\Delta t = \langle \min[\tau_{\rm GW}/(N_m + 1), t_S, t_0] \rangle$, where $\tau_{\rm GW}$ is given by Eq. (2); $t_S = 4.5 \times 10^8 \, {\rm yr}\eta/[f_{\rm Edd}(1 - \eta)]$ is the typical accretion "Salpeter" time scale, which depends on the Eddington ratio $f_{\rm Edd}$ and on the spin-dependent radiative efficiency η; $\langle ... \rangle$ denotes an average weighted by the Eddington-ratio probability distribution; and N_m is the average number of mergers in the interval $[t(z) - \frac{1}{2}\tau_{\rm GW}$, $t(z) + \frac{1}{2}\tau_{\rm GW}]$ [40]. Moreover, since our calculation assumes that the instability saturates before GW emission takes place, our stochastic background calculation only includes BHs for which the expected number of mergers during the instability time scale is $N_m < 1$, and for which $\tau_{\rm inst} < \Delta t$ (thus ensuring that the instability time-scale is shorter than the typical accretion and merger time scales).

The SNR for the stochastic background is [73]

$$\rho_{\rm stoch} = \sqrt{T_{\rm obs} \int_{f_{\rm min}}^{f_{\rm max}} df \frac{\Omega_{\rm GW}^2}{\Omega_{\rm sens}^2}}, \qquad (7)$$

where $\Omega_{\rm sens}^{\rm LIGO} = (S_h(f)/\sqrt{2}\Gamma_{IJ}(f))(2\pi^2/3H_0^2)f^3$ and $\Omega_{\rm sens}^{\rm LISA} = S_h(f)(2\pi^2/3H_0^2)f^3$ for LIGO [74] and LISA [75], respectively. In the LIGO case we assume the same S_h for the Livingston and Hanford detectors, and Γ_{IJ} denotes their overlap reduction function [73].

The order of magnitude of the stochastic background shown in Fig. 2 (left panel) can be estimated by a simple back-of-the-envelope calculation. The average mass fraction of an isolated BH emitted by the boson cloud is $f_{\rm ax} \sim \mathcal{O}(1\%)$ [40].
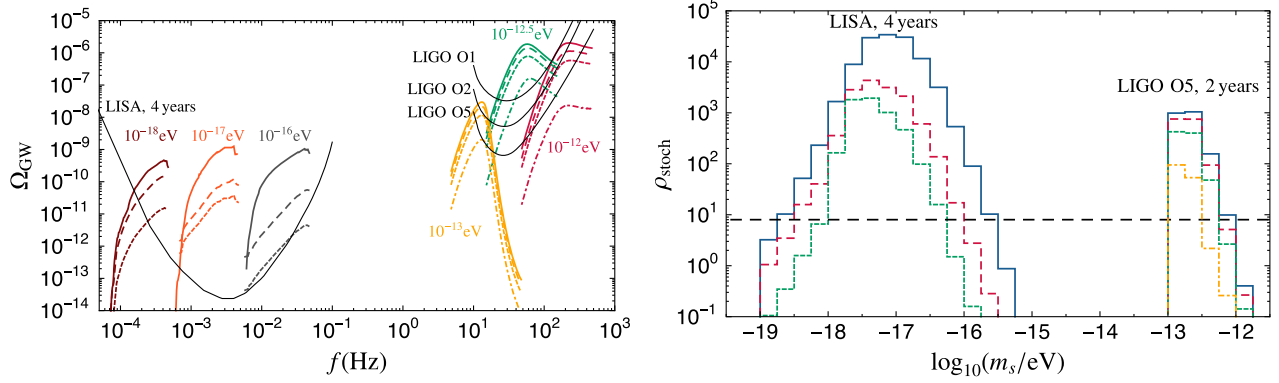
FIG. 2.   Left panel: Stochastic background in the LIGO and LISA bands. For LISA, the three different signals correspond to the optimistic (top), less optimistic (middle), and pessimistic (bottom) astrophysical models. For LIGO, the different spectra for each boson mass correspond to a uniform spin distribution with (from top to bottom) $\chi_i \in [0.8, 1]$, $[0.5, 1]$, $[0, 1]$, and $[0, 0.5]$. The black lines are the power-law integrated curves of Ref. [73], computed using noise PSDs for LISA [12], LIGO's first two observing runs (O1 and O2), and LIGO at design sensitivity (O5) [76]. By definition, $\rho_{\text{stoch}} > 1$ ($\rho_{\text{stoch}} = 1$) when a power-law spectrum intersects (is tangent to) a power-law integrated curve. Right panel: ρ_{stoch} for the backgrounds shown in the left panel. We assumed $T_{\text{obs}} = 2$ yr for LIGO and $T_{\text{obs}} = 4$ yr for LISA.

Because the signal is almost monochromatic, the emitted GWs in the detector frame span about a decade in frequency, i.e., $\Delta \ln f \sim 1$ for both LISA and LIGO (cf. Fig. 2). Thus, $\Omega_{\text{GW,ax}} = (1/\rho_c)(d\rho_{\text{GW}}/d\ln f) \sim f_{\text{ax}}\rho_{\text{BH}}/\rho_c$, where ρ_{GW} and ρ_{BH} are the GW and BH energy density, respectively. Since the BH mass density is $\rho_{\text{BH}} \sim \mathcal{O}(10^4) M_{\odot}/\text{Mpc}^3$ in the mass range $10^4 - 10^7\ M_{\odot}$ relevant for LISA, this yields $\Omega_{\text{GW,ax}}^{\text{LISA}} \sim 10^{-9}$. For LIGO, the background of GWs from BH binaries can be approximated as $\Omega_{\text{GW,bin}} \sim f_{\text{GW}}f_m\rho_{\text{BH}}/\rho_c$, where $f_{\text{GW}} \sim \mathcal{O}(1\%)$ is the binary's mass fraction emitted in GWs [77], and $f_m \sim \mathcal{O}(1\%)$ [54] is the fraction of stellar-mass BHs in binaries that merge in less than t_0. Therefore, $\Omega_{\text{GW,ax}}/\Omega_{\text{GW,bin}} \sim f_{\text{ax}}/(f_{\text{GW}}f_m) \sim 10^2$. Since the O1 results imply peak background values $\Omega_{\text{GW,bin}} \sim 10^{-9} - 10^{-8}$ [76,78] (or larger if spins are included), we obtain $\Omega_{\text{GW,ax}}^{\text{LIGO}} \sim 10^{-7} - 10^{-6}$. These estimates are in qualitative agreement with the left panel of Fig. 2.

Remarkably, ρ_{stoch} (right panel of Fig. 2) can be very high. For optimistic astrophysical models, boson masses in the range 2×10^{-13} eV $\lesssim m_s \lesssim 10^{-12}$ eV (5×10^{-19} eV $\lesssim m_s \lesssim 5 \times 10^{-16}$ eV) yield $\rho_{\text{stoch}} > 8$ with LIGO (LISA). Our estimates suggest that, for the most pessimistic model and masses around $m_s \approx 3 \times 10^{-12}$ eV, the background would have SNR ≈ 1.2 using our simple analytic estimate of the LIGO O1 sensitivity, thus being only marginally allowed by current LIGO O1 upper limits [78]. Our conclusions should be validated by a careful data analysis of the stochastic background in LIGO O1 and O2. In particular, current upper limits on the stochastic background assume that the spectrum can be described by a power law in the LIGO range [78], which is not the case for the backgrounds computed here.

Resolvable sources.—We estimate the number of resolvable events as [40]

$$N = \int_{\rho > 8} \frac{d^2\dot{n}}{dM d\chi}\left(\frac{T_{\text{obs}}}{1 + z} + \Delta t\right)\frac{dV_c}{dz}dzdMd\chi, \quad (8)$$

where $dV_c = 4\pi D_c^2 dD_c$, D_c is the comoving distance, and $\dot{n} = n/t_0$ for LISA. The dependence on $T_{\text{obs}}/(1 + z) + \Delta t$ comes about because the probability that an observation of duration T_{obs} and a signal of duration $\Delta t(1 + z)$ (in the detector frame) overlap is proportional to the sum of the two durations. In the limit $\Delta t(1 + z) \ll T_{\text{obs}}$ we have $N \propto T_{\text{obs}}$, as usual for short-lived sources [79]. For $\Delta t(1 + z) \gg T_{\text{obs}}$, N becomes proportional to the duty cycle $\Delta t/t_f$, $t_f \equiv n/\dot{n}$ being the formation timescale of the boson condensates. This duty cycle, akin, e.g., to the duty cycle of active galactic nuclei, accounts for the fact that only a fraction of the sources are radiating during the observation time.

Figure 3 shows resolvable event rates assuming (conservatively) semicoherent searches for different astrophysical models. The SNR was computed by including the confusion noise from the stochastic background of unresolvable boson-condensate sources: neglecting this contribution would overestimate LISA rates by more than 1 order of magnitude. Our models typically predict ~ 40 (200) events in 121×250 h total observation time for the optimistic models and boson masses in the optimal range around $m_s \sim 10^{-17}$ eV (3×10^{-13} eV) for LISA (LIGO). Rates in the less optimistic and pessimistic models decrease by factors of order unity. However, it is remarkable that a boson with $m_s \sim 10^{-17}$ eV (3×10^{-13} eV) would produce around 5 (15) direct LISA (LIGO) detections even for pessimistic astrophysical models.

So far we focused on the *direct* detection of GWs from bosonic condensates. In Ref. [40] we use Bayesian model selection to show that LISA could infer the existence of light
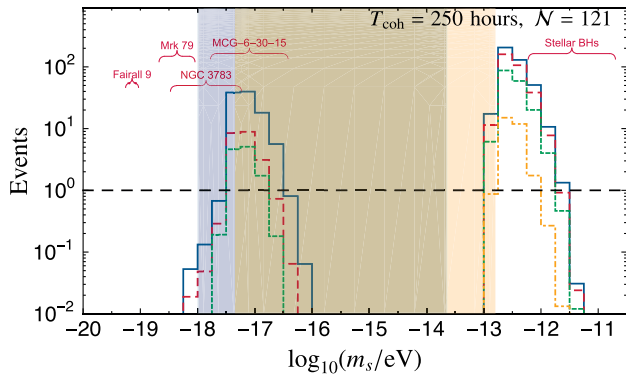
FIG. 3.   Resolvable events for the same astrophysical models used in Fig. 2. Shaded areas correspond to exclusion regions from four-year LISA massive BH spin measurements, using either the popIII (brown) or Q3-nod (light blue) models of Ref. [48]. For reference we also show with brackets the constraints that can be placed by spin measurements of massive or stellar-mass BHs [37,80].

bosons *indirectly*: LISA measurements of massive BH spins could provide evidence for holes in the BH mass-spin "Regge plane" (i.e., for the absence of BHs spinning above the superradiant instability window) [35]. As indicated by the shaded areas in Fig. 3, a four-year LISA mission could rule out boson masses in a range that depends on the assumed BH model ($[4.5 \times 10^{-18}, 1.6 \times 10^{-13}]$ for the "light-seed" popIII model, $[10^{-18}, 2.3 \times 10^{-14}]$ for the "heavy-seed, no-delay" Q3-nod model of Ref. [48]). If fields with $m_s \in [10^{-17}, 10^{-13}]$ eV exist in nature, LISA observations of BH mergers can measure m_s with 10% accuracy [40].

Conclusions.—Together, Earth- and space-based detectors will allow for multiband GW searches of ultralight bosons in the range $[10^{-19} - 10^{-10}]$ eV. We plan to improve estimates of the stochastic background for LIGO by using population synthesis models [6,81,82]. The potential of detectors like DECIGO or the Einstein Telescope to detect or rule out bosons of mass $m_s \sim 10^{-14}$ eV should also be investigated by using intermediate-mass BH formation models [47,83]. Our analysis must be extended to spin-1 [24,25] and spin-2 [30] fields, for which the instability time scales are shorter and GW amplitudes are larger. Our results also suggest that recent estimates of resolvable GWs from spin-1 instabilities [29] should be revised, taking into account the stochastic background.

[1] B. P. Abbott *et al.* (Virgo, LIGO Scientific Collaborations), Phys. Rev. Lett. **116**, 061102 (2016).
[2] B. P. Abbott *et al.* (Virgo, LIGO Scientific Collaborations), Phys. Rev. Lett. **116**, 241103 (2016).
[3] B. P. Abbott *et al.* (VIRGO, LIGO Scientific Collaborations), Phys. Rev. Lett. **118**, 221101 (2017).
[4] E. Berti, V. Cardoso, and C. M. Will, Phys. Rev. D **73**, 064030 (2006).
[5] V. Cardoso, E. Franzin, and P. Pani, Phys. Rev. Lett. **116**, 171101 (2016); Phys. Rev. Lett. **117**, 089902E (2016).
[6] E. Berti, A. Sesana, E. Barausse, V. Cardoso, and K. Belczynski, Phys. Rev. Lett. **117**, 101102 (2016).
[7] J. R. Gair, M. Vallisneri, S. L. Larson, and J. G. Baker, Living Rev. Relativ. **16**, 7 (2013).
[8] N. Yunes and X. Siemens, Living Rev. Relativ. **16**, 9 (2013).
[9] E. Berti *et al.*, Classical Quantum Gravity **32**, 243001 (2015).
[10] B. P. Abbott *et al.* (Virgo, LIGO Scientific Collaborations), Phys. Rev. Lett. **116**, 221101 (2016).
[11] J. Aasi *et al.* (LIGO Scientific Collaboration), Classical Quantum Gravity **32**, 074001 (2015).
[12] H. Audley *et al.*, arXiv:1702.00786.
[13] A. Arvanitaki, S. Dimopoulos, S. Dubovsky, N. Kaloper, and J. March-Russell, Phys. Rev. D **81**, 123530 (2010).
[14] R. Essig *et al.*, *Proceedings of the Community Summer Study 2013: Snowmass on the Mississippi (CSS2013) Minneapolis, MN, USA, 2013* (2013) [arXiv:1311.0029].
[15] D. J. E. Marsh, Phys. Rep. **643**, 1 (2016).
[16] L. Hui, J. P. Ostriker, S. Tremaine, and E. Witten, Phys. Rev. D **95**, 043541 (2017).
[17] W. H. Press and S. A. Teukolsky, Nature (London) **238**, 211 (1972).
[18] S. L. Detweiler, Phys. Rev. D **22**, 2323 (1980).
[19] V. Cardoso, O. J. C. Dias, J. P. S. Lemos, and S. Yoshida, Phys. Rev. D **70**, 044039 (2004).
[20] R. Brito, V. Cardoso, and P. Pani, Lect. Notes Phys. **906**, 1 (2015).
[21] T. J. M. Zouros and D. M. Eardley, Ann. Phys. (N.Y.) **118**, 139 (1979).

[22] V. Cardoso and S. Yoshida, J. High Energy Phys. 07 (2005) 009.

[23] S. R. Dolan, Phys. Rev. D **76**, 084001 (2007).

[24] P. Pani, V. Cardoso, L. Gualtieri, E. Berti, and A. Ishibashi, Phys. Rev. Lett. **109**, 131102 (2012).

[25] P. Pani, V. Cardoso, L. Gualtieri, E. Berti, and A. Ishibashi, Phys. Rev. D **86**, 104017 (2012).

[26] H. Witek, V. Cardoso, A. Ishibashi, and U. Sperhake, Phys. Rev. D **87**, 043513 (2013).

[27] S. Endlich and R. Penco, J. High Energy Phys. 05 (2017) 052.

[28] W. E. East and F. Pretorius, Phys. Rev. Lett. **119**, 041101 (2017).

[29] M. Baryakhtar, R. Lasenby, and M. Teo, Phys. Rev. D **96**, 035019 (2017).

[30] R. Brito, V. Cardoso, and P. Pani, Phys. Rev. D **88**, 023514 (2013).

[31] H. Okawa, H. Witek, and V. Cardoso, Phys. Rev. D **89**, 104032 (2014).

[32] M. Zilhão, H. Witek, and V. Cardoso, Classical Quantum Gravity **32**, 234003 (2015).

[33] N. Sanchis-Gual, J. C. Degollado, P. J. Montero, J. A. Font, and C. Herdeiro, Phys. Rev. Lett. **116**, 141101 (2016).

[34] P. Bosch, S. R. Green, and L. Lehner, Phys. Rev. Lett. **116**, 141102 (2016).

[35] A. Arvanitaki and S. Dubovsky, Phys. Rev. D **83**, 044026 (2011).

[36] R. Brito, V. Cardoso, and P. Pani, Classical Quantum Gravity **32**, 134001 (2015).

[37] A. Arvanitaki, M. Baryakhtar, and X. Huang, Phys. Rev. D **91**, 084011 (2015).

[38] H. Yoshino and H. Kodama, Prog. Theor. Exp. Phys. (2015) 061E01.

[39] A. Arvanitaki, M. Baryakhtar, S. Dimopoulos, S. Dubovsky, and R. Lasenby, Phys. Rev. D **95**, 043001 (2017).

[40] R. Brito, S. Ghosh, E. Barausse, E. Berti, V. Cardoso, I. Dvorkin, A. Klein, and P. Pani, arXiv:1706.06311 [Phys. Rev. D (to be published)].

[41] S. A. Teukolsky, Astrophys. J. **185**, 635 (1973).

[42] H. Yoshino and H. Kodama, Prog. Theor. Exp. Phys. (**2014**) 043E02.

[43] E. Berti, A. Buonanno, and C. M. Will, Phys. Rev. D **71**, 084025 (2005).

[44] C. Palomba, (VIRGOLIGO Scientific Collaborations), in *Proceedings of the 46th Rencontres de Moriond on Gravitational Waves and Experimental Gravity: La Thuile Italy, March 20–27, 2011* (2012), p. 27; arXiv:1201.3176

[45] A. J. Ruiter, K. Belczynski, M. Benacquista, S. L. Larson, and G. Williams, Astrophys. J. **717**, 1006 (2010).

[46] B. P. Abbott *et al.* (VIRGO, LIGO Scientific Collaborations), Living Rev. Relativ. **19**, 1 (2016).

[47] S. Kawamura *et al.*, Classical Quantum Gravity **23**, S125 (2006).

[48] A. Klein *et al.*, Phys. Rev. D **93**, 024003 (2016).

[49] S. Babak, J. Gair, A. Sesana, E. Barausse, C. F. Sopuerta, C. P. L. Berry, E. Berti, P. Amaro-Seoane, A. Petiteau, and A. Klein, Phys. Rev. D **95**, 103012 (2017).

[50] E. Barausse, Mon. Not. R. Astron. Soc. **423**, 2533 (2012).

[51] A. Sesana, E. Barausse, M. Dotti, and E. M. Rossi, Astrophys. J. **794**, 104 (2014).

[52] F. Antonini, E. Barausse, and J. Silk, Astrophys. J. **812**, 72 (2015).

[53] F. Antonini, E. Barausse, and J. Silk, Astrophys. J. **806**, L8 (2015).

[54] I. Dvorkin, E. Vangioni, J. Silk, J. P. Uzan, and K. A. Olive, Mon. Not. R. Astron. Soc. **461**, 3877 (2016).

[55] E. Vangioni, K. A. Olive, T. Prestegard, J. Silk, P. Petitjean, and V. Mandic, Mon. Not. R. Astron. Soc. **447**, 2575 (2015).

[56] R. J. Bouwens, G. D. Illingworth, P. A. Oesch, I. Labbé, M. Trenti, P. van Dokkum, M. Franx, M. Stiavelli, C. M. Carollo, D. Magee, and V. Gonzalez, Astrophys. J. **737**, 90 (2011).

[57] P. S. Behroozi, R. H. Wechsler, and C. Conroy, Astrophys. J. **770**, 57 (2013).

[58] E. E. Salpeter, Astrophys. J. **121**, 161 (1955).

[59] D. Schaerer, Astron. Astrophys. **382**, 28 (2002).

[60] S. E. Woosley and T. A. Weaver, Astrophys. J. Suppl. Ser. **101**, 181 (1995).

[61] J. S. Vink, New Astron. **52**, 419 (2008).

[62] S. E. de Mink, M. Cantiello, N. Langer, O. R. Pols, I. Brott, and S. C. Yoon, Astron. Astrophys. **497**, 243 (2009).

[63] C. L. Fryer, K. Belczynski, G. Wiktorowicz, M. Dominik, V. Kalogera, and D. E. Holz, Astrophys. J. **749**, 91 (2012).

[64] P. S. Behroozi, R. H. Wechsler, and C. Conroy, Astrophys. J. Lett. **762**, L31 (2013).

[65] X. Ma, P. F. Hopkins, C. A. Faucher-Giguère, N. Zolman, A. L. Muratov, D. Kereš, and E. Quataert, Mon. Not. R. Astron. Soc. **456**, 2140 (2016).

[66] L. Hernquist, Astrophys. J. **356**, 359 (1990).

[67] S. Shen, H. J. Mo, S. D. M. White, M. R. Blanton, G. Kauffmann, W. Voges, J. Brinkmann, and I. Csabai, Mon. Not. R. Astron. Soc. **343**, 978 (2003).

[68] C. Porcel, F. Garzon, J. Jimenez-Vicente, and E. Battaner, Astron. Astrophys. **330**, 136 (1998).

[69] E. S. Phinney, arXiv:astro-ph/0108028.

[70] D. Gerosa and E. Berti, Phys. Rev. D **95**, 124046 (2017).

[71] M. Fishbach, D. E. Holz, and B. Farr, Astrophys. J. **840**, L24 (2017).

[72] A. R. King and U. Kolb, Mon. Not. R. Astron. Soc. **305**, 654 (1999).

[73] E. Thrane and J. D. Romano, Phys. Rev. D **88**, 124032 (2013).

[74] B. Allen and J. D. Romano, Phys. Rev. D **59**, 102001 (1999).

[75] N. J. Cornish and S. L. Larson, Classical Quantum Gravity **18**, 3473 (2001).

[76] B. P. Abbott *et al.* (Virgo, LIGO Scientific), Phys. Rev. Lett. **116**, 131102 (2016).

[77] E. Barausse, V. Morozova, and L. Rezzolla, Astrophys. J. **758**, 63 (2012); Astrophys. J. **786**, 76E (2014).

[78] B. P. Abbott *et al.* (Virgo, LIGO Scientific Collaborations), Phys. Rev. Lett. **118**, 121101 (2017).

[79] T. Hartwig, M. Volonteri, V. Bromm, R. S. Klessen, E. Barausse, M. Magg, and A. Stacy, Mon. Not. R. Astron. Soc. **460**, L74 (2016).

[80] L. Brenneman, C. Reynolds, M. Nowak, R. Reis, M. Trippe *et al.*, Astrophys. J. **736**, 103 (2011).

[81] K. Belczynski *et al.*, Astron. Astrophys. **594**, A97 (2016).

[82] K. Belczynski, T. Ryu, R. Perna, E. Berti, T. L. Tanaka, and T. Bulik, arXiv:1612.01524.

[83] J. R. Gair, I. Mandel, M. C. Miller, and M. Volonteri, Gen. Relativ. Gravit. **43**, 485 (2011).